

文章编号: 0258-1825(2010)06-0645-05

## Research on the RCS of hypervelocity model and its plasma sheath

ZENG Xue-jun<sup>1</sup>, YU Zhe-feng<sup>2</sup>, BU Shao-qing<sup>2</sup>, LIU Sen<sup>2</sup>,  
MA Ping<sup>2</sup>, SHI An-hua<sup>2</sup>, LIANG Shi-chang<sup>2</sup>

1. Northwestern Polytechnical University, Xi'an 710072, China;

2. China Aerodynamics Research and Development Center, Mianyang Sichuan 621000, China)

**Abstract:** The scattering characteristics of hypervelocity models are measured in the aero-physics range of CARDC (China Aerodynamics Research and Development Center) to research reentry electromagnetic phenomenology. The received radar signal and one-dimensional RCS image of hypervelocity models are obtained. According to these experiments, three-dimensional (3-D) finite-difference time-domain (FDTD) simulations are performed. The numerical results are in reasonable agreement with the experimental results. The simulating results also show the RCS of hypervelocity models will be changed obviously by the deviation of the incident radar wave angle.

**Key words:** reentry; RCS; plasma; hypervelocity

中图分类号: V211.753

文献标识码: A

### 0 Introduction

When a space vehicle reenters the atmosphere, its scattering characteristics will be significantly changed by the formation of an ionized shock layer. The flow of the gas in the shock layer is characterized by ionized air and ablation of the mass of the body. The chemical kinetics of the ionized shock layer is very complicated. The Radar Cross Section (RCS) of the space vehicle may be decreased or increased due to a number of effects associated with the plasma sheath. The effects of the plasma sheath will occur at certain combinations of altitude and speed<sup>[1-3]</sup>.

Instrumented aero-physics ranges have made major contributions to the understanding of reentry phenomenology through many experiments performed under controlled test conditions. Some accomplishments have been reported in the open literature since 1967<sup>[4]</sup>.

Other researchers studied reentry phenomenology

by theoretic analysis and numerical simulation. The exact calculation of the RCS of a hypersonic vehicle is a very difficult problem. In principle, the procedure for making this calculation would be, first, to determine the configuration and properties of the plasma sheath and surrounding atmosphere. With the electron density and collision frequency in the plasma determined thereby, the electromagnetic properties of the sheath are specified and the distribution of the complex dielectric constant about the object is determined. Given this distribution, the shape and material of the space vehicle, Maxwell's equations with appropriate boundary conditions would have to be solved.

In this paper, the RCS measurements of hypervelocity models in the aero-physics range of CARDC are introduced. The received signal and one-dimensional radar image of hypervelocity models are obtained. According to these experiments, three-dimensional FDTD simulations are performed.

\* 收稿日期: 2009-03-17; 修訂日期: 2009-09-11

基金项目: 国家自然科学基金(109020120)

作者简介: 曾学军(1962-), 男, 四川省大英县人, 研究员, 研究方向: 再入物理、目标特性.

## 1 The experiment in aero-physics range

To research the effects of the plasma sheath, the RCS of hypervelocity models are measured in the aero-physics range of CARDC.

### 1.1 RCS measure systems

The sketch map of the hypervelocity models and reference frame is shown in Fig. 1.

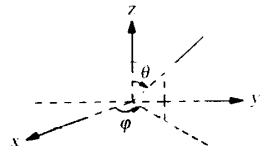


Fig. 1 Experimental model

图1 试验模型

There are two RCS measure systems in this aero-physics range. One operates at  $X$  band and the other operates at  $Ka$  band. To  $X$  band radar, monostatic RCS may be measured. The incident direction of electromagnetic wave is  $\theta=45^\circ$ ,  $\varphi=90^\circ$  while the reflected direction of electromagnetic wave is  $\theta=135^\circ$ ,  $\varphi=-90^\circ$ . To  $Ka$  band radar, bistatic RCS may be measured. The incident direction of electromagnetic wave is  $\theta=0^\circ$ ,  $\varphi=90^\circ$  while the reflected direction of electromagnetic wave is  $\theta=113^\circ$ ,  $\varphi=-90^\circ$ . The antennas' positions are shown in Fig. 2.

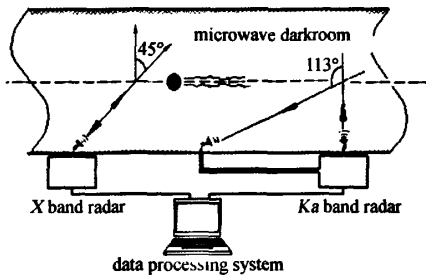


Fig. 2 Antennas' positions

图2 天线位置

The  $X$  band and  $Ka$  band radars will receive the scattering signals when a hypervelocity model passes the microwave darkroom. By near to far transition, One-dimensional RCS image and total RCS will be obtained.

### 1.2 Experimental results

In the experiment, the diameter of hypervelocity model is 10mm. The velocity of these hypervelocity models is accelerated to 4.5km/s by two stage light gas

gun. The pressure is 20.0kPa in the microwave darkroom.

The received Doppler signal and its spectrum at  $X$  band are shown in Fig. 3 and Fig. 4.

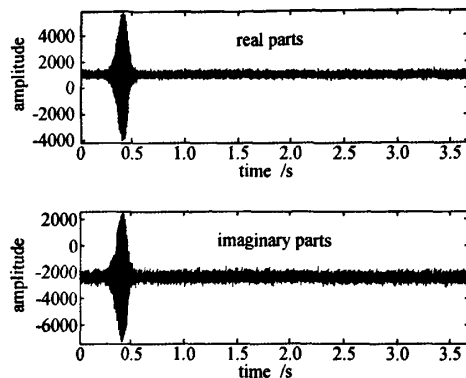


Fig. 3 Received Doppler signal at  $X$  band  
图3  $X$  波段雷达接收到的 Doppler 信号

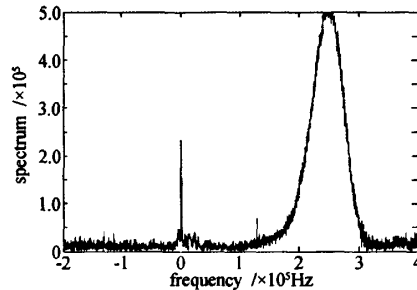


Fig. 4 Spectrum of received signal at  $X$  band  
图4  $X$  波段雷达接收信号频谱

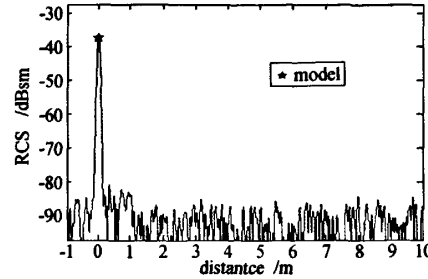


Fig. 5 One-dimensional RCS image at  $X$  band  
图5  $X$  波段 RCS 一维距离像

The received Doppler signal and its spectrum at  $Ka$  band are shown in Fig. 6 and Fig. 7.

One-dimensional RCS image of the model at  $Ka$  band is shown in Fig. 8. The RCS of this model and its plasma sheath is  $-43.9$  dBsm. As can be seen from Fig. 8, the scattering center is the bottom of this model.

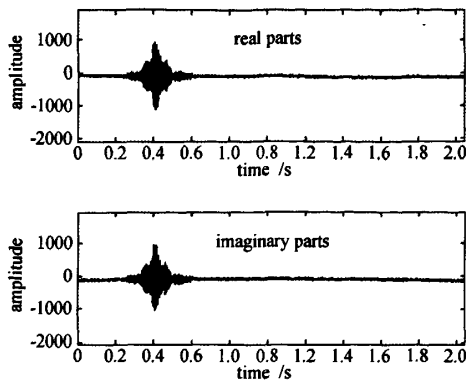


Fig. 6 Received Doppler signal at Ka band  
图6 Ka波段雷达接收到的Doppler信号

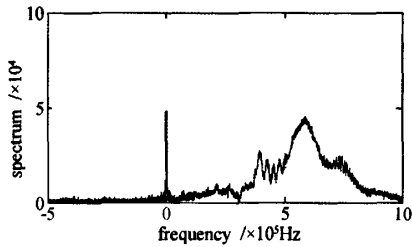


Fig. 7 Spectrum of received signal at Ka band  
图7 Ka波段雷达接收信号频谱

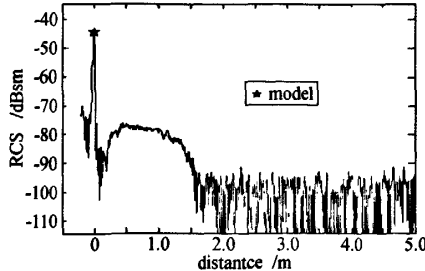


Fig. 8 One-dimensional RCS image at Ka band  
图8 Ka波段RCS一维距离像

## 2 Flow field simulating

High-temperature chemically non-equilibrium equations are solved to determine the configuration and properties of the plasma sheath<sup>[6]</sup>. The equations are:

$$\frac{\partial Q}{\partial t} + \frac{\partial F}{\partial x} + \frac{\partial G}{\partial y} + \frac{\partial H}{\partial z} = \frac{1}{Re} \left( \frac{\partial F_V}{\partial x} + \frac{\partial G_V}{\partial y} + \frac{\partial H_V}{\partial z} \right) + W \quad (1)$$

where,

$$Q = \begin{bmatrix} \rho_i \\ \rho E_V \\ \rho \\ \rho u \\ \rho v \\ \rho w \\ \rho E \end{bmatrix}, \quad F = \begin{bmatrix} \rho u \\ \rho E_V \\ \rho u \\ \rho u^2 + p \\ \rho uv \\ \rho uw \\ (\rho E + p)u \end{bmatrix},$$

$$F_V = \begin{bmatrix} \rho D_i \frac{\partial c_i}{\partial x} \\ q_{Vx} \\ 0 \\ \tau_{xx} \\ \tau_{yy} \\ \tau_{zz} \\ q_x + u_j \tau_{sj} \end{bmatrix}, \quad W = \begin{bmatrix} w_i \\ w_V \\ 0 \\ 0 \\ 0 \\ 0 \\ 0 \end{bmatrix} \quad (2)$$

A program is made to solve these equations. According to the experiment described above, the electron density and collision frequency of plasma sheath are obtained by this program.

## 3 RCS simulating

3-D FDTD is used to calculate the microwave scattering characteristics of hypervelocity models and its plasma sheath.

Plasma can be looked as a kind of dispersive medium<sup>[4-5]</sup>. To simulate the electromagnetic characteristics of plasma by FDTD, some methods such as Direct Integration (DI), recursive convolution (RC) and Z-transform may be used to build the dispersive constitutive relation. In this paper, DI method of FDTD is used to research the scattering characteristic of three dimensional plasma-cloaked targets.

The relative permittivity of nonmagnetized cold plasma is complex and given by

$$\epsilon_r = 1 - \frac{\omega_p^2}{\omega^2 + \nu_c^2} - i \frac{\nu_c}{\omega} \frac{\omega_p^2}{\omega^2 + \nu_c^2} \quad (3)$$

where  $\omega$  is angular frequency of EM fields,  $\nu_c$  is the collision frequency of plasma and  $\omega_p = (n_e e^2 / m_e \epsilon_0)^{1/2}$  is the angular frequency of plasma, where  $e$  and  $m_e$  are electron charge and mass,  $n_e$  is electron number density, and  $\epsilon_0$  is free-space permittivity.

According to Young's DI method, Maxwell's equation can be written as:

$$J_x |_{i,j,k}^{n+1/2} = \frac{1 - \nu \Delta t / 2}{1 + \nu \Delta t / 2} J_x |_{i,j,k}^{n-1/2} + \frac{2 \epsilon_0 \Delta t}{2 + \nu \Delta t} \omega_p^2 |_{i,j,k}^n \quad (4)$$

$$E_x |_{i+1/2,j,k}^{n+1} = E_x |_{i+1/2,j,k}^n + \frac{1}{\epsilon_0} \left[ \frac{\Delta t}{\Delta y} (H_z |_{i+1/2,j+1/2,k}^{n+1/2} - H_z |_{i+1/2,j-1/2,k}^{n+1/2}) \right] - \frac{1}{\epsilon_0} \left[ \frac{\Delta t}{\Delta z} (H_y |_{i+1/2,j,k+1/2}^{n+1/2} - H_y |_{i+1/2,j,k-1/2}^{n+1/2}) \right] - \frac{\Delta t}{2 \epsilon_0} (J_x |_{i+1/2,j,k}^{n+1/2} - J_x |_{i,j,k}^{n+1/2}) \quad (5)$$

$$H_x |_{i,j+1/2,k+1/2}^{n+1/2} = H_x |_{i,j+1/2,k+1/2}^{n-1/2} - \frac{1}{\mu_0} \left[ \frac{\Delta t}{\Delta y} (E_z |_{i,j+1/2,k+1/2}^n - E_z |_{i,j,k+1/2}^n) \right] + \frac{1}{\mu_0} \left[ \frac{\Delta t}{\Delta z} (E_y |_{i,j+1/2,k+1/2}^n - E_y |_{i,j,k+1/2}^n) \right] \quad (6)$$

It's a second-order accurate approximation. This method only requires the storage of one time level of each field component, and uses significantly fewer multiply and add operations per time step than the other methods.

To verify the Direct Integration Method which is described above, the RCS of plasma sphere was computed for comparison with the result of Mie's method, where the radius of plasma sphere  $r=0.2\text{m}$ , the incident wave frequency  $f=1.0\text{GHz}$ , angular frequency of plasma  $\omega_p=3.0\text{GHz}$ , collision frequency  $\nu_c=1.0\text{GHz}$ . As can be seen from Fig. 9 and Fig. 10, in H plane and E plane, the agreement is good at all angles.

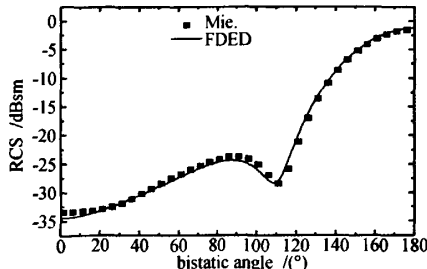


Fig. 9 RCS of plasma sphere (H plane)  
图9 等离子体球的 RCS(H 平面)

According to the experimental conditions, in implementing the FDTD scheme, a cell size of  $dx=dy=dz=0.133\text{mm}$  is employed. The circumferences of the model are approximated with the staircase grids.

When the incident direction of electromagnetic wave is  $\theta=45^\circ$ ,  $\varphi=90^\circ$  and the reflected direction of

electromagnetic wave is  $\theta=135^\circ$ , the bistatic RCS of this model at X band versus angle  $\varphi$  is shown in Fig. 11.

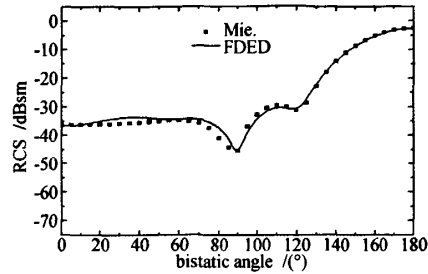


Fig. 10 RCS of plasma sphere (E plane)  
图10 等离子体球的 RCS(E 平面)

When the incident direction of electromagnetic wave is  $\theta=0^\circ$ ,  $\varphi=90^\circ$  and the reflected direction of electromagnetic wave is  $\theta=113^\circ$ , the RCS of this model at Ka band versus angle  $\varphi$  is shown in Fig. 12.

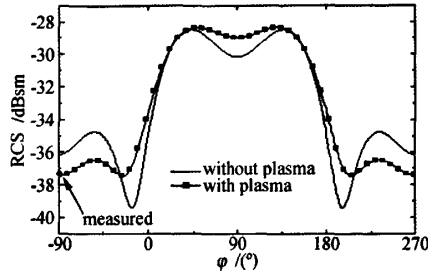


Fig. 11 Bistatic RCS at X band  
图11 X 波段双站 RCS

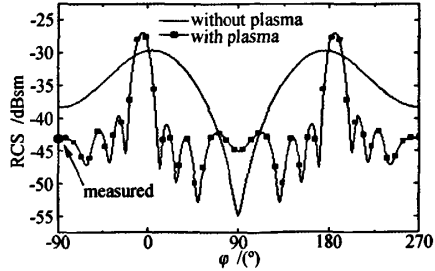


Fig. 12 Bistatic RCS at Ka band  
图12 Ka 波段双站 RCS

AS can be seen from Fig. 11 and Fig. 12, when the model is surrounded by plasma, its RCS is changed at X and Ka band. The numerical result is in reasonable agreement with the experimental results. The difference between them is less than 1dBsm.

A number of mechanisms have been proposed to explain the changes that have been observed<sup>[11]</sup>. Among these is, first, a diverging lens type of effect, where a

photo-ionized cloud preceding the sheath acts to divert the incident radar signal around the object. Second, the plasma sheath, at certain combinations of altitude and speed, may act as an absorbent coating. Third, the inhomogeneous plasma sheath may present to the incident radar wave a reflecting surface having, because of its shape, a lower cross section than the original body surface.

A lot of simulations are done to analyze the effects of the deviation of radar wave angle, flow field boundary selection and collision frequency on the RCS of the hypervelocity model. The analysis results show that the RCS of this scale model will be changed obviously by the deviation of the incident radar wave angle. Flow field boundary condition selection and collision frequency calculated by different formulae have a little effect on the RCS.

#### 4 Conclusions

To research the effects of the plasma sheath, the RCS of hypervelocity models are measured in aero-physics range of CARDC. According to these experiments, three-dimensional FDTD simulations are performed. The numerical results are in reasonable agreement with the experimental results. The analysis results also show

that the RCS of hypervelocity models will be changed obviously by the deviation of the incident angle. Flow field boundary condition selection and collision frequency calculated by different formula have a little effect on the RCS.

#### References:

- [1] JOHN W M, et al. On the decrease of the radar cross section of the apollo command module due to reentry plasma effects[R]. NASA TN D-4784.
- [2] IAMESP R, CHURCHILL W J. Progress in reentry communications[J]. *IEEE Transaction on Aerospace and Electronic Systems*, 1971, 7:879-894.
- [3] RICHARD A H. The application of instrumented light gas gun facilities for hypervelocity aerophysics research [R]. AIAA-92-3998.
- [4] LUEBBERS R J, et al. A frequency dependent finite difference time domain formulation for dispersive materials[J]. *IEEE Trans. EMC*, 1990, 32(3):222-227.
- [5] BHASKAR C, SHASHANK C. Three-dimensional computation of reduction in radar cross section using plasma shielding[J]. *IEEE Trans. on Plasma Sci.*, 2005, 33(6): 2027-2034.
- [6] GAO T S, DONG W Z, ZHANG Q Y. The computation and analysis of hypersonic flow over reentry vehicles with ablation[J]. *ACTA Aerodynamica Sinica*, 2007, (1): 3-8.

## 超高速模型及其等离子体鞘套 RCS 特性研究

曾学军<sup>1</sup>,于哲峰<sup>2</sup>,邵绍清<sup>2</sup>,柳森<sup>2</sup>,马平<sup>2</sup>,石安华<sup>2</sup>,梁世昌<sup>2</sup>

(1. 西北工业大学,陕西 西安 710072; 2. 中国空气动力研究与发展中心,四川 绵阳 621000)

**摘要:**为了研究等离子体对超高速模型雷达散射截面的影响,利用气动物理靶测量超高速模型及其绕流的雷达散射截面(RCS),给出了雷达接收信号、信号频谱和模型雷达散射截面的一维距离像。利用时域有限差分方法(FDTD)分析了等离子体鞘套对模型电磁散射特性的影响。将数值模拟结果和试验结果进行了对比,对比结果显示二者符合得很好。数值模拟结果还表明雷达入射角小角度偏移对测量结果有较大影响。

**关键词:**再入;雷达散射面积;等离子体;超高速

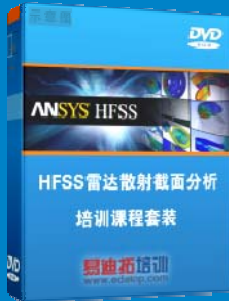
## 雷达散射截面 (RCS) 分析培训课程

易迪拓培训([www.edatop.com](http://www.edatop.com))由数名来自于研发第一线的资深工程师发起成立, 致力和专注于微波、射频、天线设计研发人才的培养, 是国内最大的微波射频和天线设计人才培养基地。客户遍布中兴通讯、研通高频、国人通信等多家国内知名公司, 以及台湾工业技术研究院、永业科技、全一电子等多家台湾地区企业。

雷达散射截面 (Radar Cross Section, 简称 RCS) 是雷达隐身技术中最关键的概念, 也是电磁理论研究的重要课题, 使用 HFSS 软件可以很方便的分析计算各种目标物体的 RCS。

由易迪拓培训推出的《HFSS 雷达散射截面分析培训课程套装》是从零讲起, 系统地向您讲授如何使用 HFSS 软件进行雷达散射截面分析的全过程。该套视频课程由专家讲授, 边操作边讲解, 直观易学。

### HFSS 雷达散射截面分析培训课程套装



套装包含两门视频培训课程, 其中: 《两周学会 HFSS》培训课程是作为 HFSS 的入门培训课程, 帮助您在最短的时间内迅速熟悉、掌握 HFSS 的实际操作和工程应用; 《HFSS 雷达散射截面(RCS)分析》培训课程是专门讲授如何使用 HFSS 来分析计算雷达散射截面, 包括雷达散射截面、单站 RCS、双站 RCS 等的定义, 实例讲解使用 HFSS 分析单站 RCS、双站 RCS 和宽频 RCS 的相关设置和实际操作等。视频课程, 专家讲授, 从零讲起, 直观易学...

课程网址: <http://www.edatop.com/peixun/hfss/130.html>

### ● 更多培训课程:

#### ● HFSS 培训课程

网址: <http://www.edatop.com/peixun/hfss/>

#### ● CST 培训课程

网址: <http://www.edatop.com/peixun/cst/>

#### ● 天线设计培训课程

网址: <http://www.edatop.com/peixun/antenna/>